Scientia Iranica A (2013) 20(6), 1676–1684

SCIENTIA IRANICA

Sharif University of Technology
Scientia Iranica
Transactions A: Civil Engineering
www.scientiairanica.com

Nonlinear dynamic analysis of a concrete gravity dam considering an elastoplastic constitutive model for the foundation

S.M. Aghajanzadeh and M. Ghaemian*

Department of Civil Engineering, Sharif University of Technology, Tehran, P.O. Box 11155-9313, Iran.

Received 18 February 2013; received in revised form 28 April 2013; accepted 21 May 2013

KEYWORDS
Foundation's elastoplastic behavior; Nonlinear dynamic analysis; Mohr-Coulomb model; Smeared crack model; Seismic analysis; Concrete gravity dam.

Abstract. Dam failure can result in a catastrophic break followed by a flood wave, often with considerable loss of life or property. One of the main causes of dam failure is loss of shear strength and the existence of discontinuity within the foundation. Dynamic analysis of concrete dams usually considered concrete behavior to be nonlinear and the foundation rock is assumed to be linear. In this study, seismic analysis of a concrete gravity dam was conducted to investigate the effect of the foundation on the nonlinear response. A finite element model of a dam-reservoir-foundation was considered to properly model the foundation as well as dam body nonlinear behaviors. An elasto-plastic formulation was used to model the foundation. The Mohr-Coulomb model was utilized for the yield and potential functions of the foundation. The dam body was modeled using a smeared crack model. After modeling the dam-reservoir foundation, the horizontal recorded ground acceleration of the Kobe 1995 earthquake was applied to the model and results were studied. It was found that cracks form at the crest and hill of the dam. Using the elastoplastic model for the foundation is more realistic, and under different boundary conditions, a significant amount of energy will be dissipated in the foundation.

1. Introduction

Concrete dams are an important part of nation's infrastructure. They store water for different purposes, such as irrigation, water supply, flood control, electric power, recreation and the improvement of navigation. The safety of concrete dams is a major challenge for owners due to its possible failure consequences when subjected to severe earthquake ground motion. Therefore, it is required to determine the concrete gravity dam's response under different earthquake ground motion in high seismic zones. Rescher (1990) indicated that most concrete gravity dams will experience cracking even under operational loading condition [1]. Therefore, the assumption of linear behavior may not be appropriate in the analysis of the seismic response of concrete gravity dams, and nonlinear dynamic analysis needs to be carried out for dam-reservoir-foundation systems. The nonlinear dynamic response of concrete dams depends on their interaction with the reservoir and foundation, and the approach to modeling these interactions depends on the constitutive models considered for their materials.

Dam-foundation interaction has been the topic of many studies. Motamedi et al. (2008) studied the effect of the foundation on the seismic behavior of concrete dams. They concluded that considering a rigid foundation affects the behavior of a concrete dam, and the model with a massless foundation is very conservative. Their dynamic finite element analysis

*. *Corresponding author. Tel.: +98 21 66164242; Fax: +98 21 66014828*
E-mail address: ghaemian@sharif.edu (M. Ghaemian)

resulted that incorporating the dam-foundation rock interaction is dependent on the dam and foundation modulus used in the analysis [2]. Sarkar et al. (2007) studied the effect of the foundation on the nonlinear behavior of concrete dams. Accordingly, they found that the results of their analysis related to foundation and reservoir interaction. They concluded that by reducing foundation modules, deformation increases [3]. Arabshahi and Lotfi (2008) investigated the earthquake response of concrete gravity dams, including dam-foundation interface nonlinearities. Their results show that sliding generally reduces the maximum amount of tensile principal stresses in the dam body, although there are some cracks in the body of the dam [4]. Fishman (2008) studied the shear failure of brittle materials and concrete structures on the rock foundation. It was concluded that the failure of brittle materials by shear takes place, along with weak surfaces, characterized by both low values of shear strength ($\varnothing$ and C) and low levels of normal stresses. Using this model, the cause of the serious Malpasset dam failure in France was investigated, too [5].

In this study, the dynamic nonlinear analysis of a dam-reservoir-foundation is carried out to obtain the dam response, considering foundation nonlinearity as well as dam body nonlinearity. The main purpose of this study is to predict the behavior of concrete gravity dams under seismic loads, considering an elastoplastic model of the foundation.

2. Coupled equation of dam-reservoir-foundation

The coupled dam-reservoir equations are represented as follows:

$$[M]\{\ddot{u}\} + [C]\{\dot{u}\} + [K]\{u\} = \{f_1\} - [M]\{\ddot{u}_g\} + [Q]\{p\} = \{F_1\} + [Q]\{p\}, \quad (1)$$

$$[G]\{\ddot{p}\} + [C']\{\dot{p}\} + [K']\{p\} = \{f_2\} - \rho[Q]^T(\{\ddot{u}\} + \{\ddot{u}_g\}) = \{F_2\} - \rho[Q]^T\{\ddot{u}\}, \quad (2)$$

where $[M]$, $[C]$ and $[K]$ are mass, damping and stiffness matrices of the structure, including the body of the dam and foundation, and $[G]$, $[C']$ and $[K']$ are matrices representing the mass, damping and stiffness of the reservoir, respectively. $[Q]$ is the coupling matrix; $\{f_1\}$ is the vector of the body force and hydrodynamic force; $\{F_2\}$ is the component of the force due to acceleration at the boundaries of the dam-reservoir and reservoir-foundation; and $\{p\}$ and $\{u\}$ are the vector of hydrodynamic pressures and displacements. $\{\ddot{u}_g\}$ are the ground acceleration and ρ is the density of the fluid. The dot represents the time derivative. For solving dam-reservoir-foundation interaction, the staggered displacement solution scheme was used [6].

3. Material behavior

A dam body and foundation are assumed to behave elastically at the start of the analysis. No linear constitutive models are used for the dam body and foundation when they go beyond the elastic region. A computer code was developed in this study for considering a dynamic constitutive model for the foundation and concrete.

3.1. Concrete and foundation in elastic region

Hook's law is used for determining the response of the structure in the elastic region as below:

$$\{\sigma\} = [D]\{\varepsilon\}, \quad (3)$$

where $[D]$ is the module matrix, $\{\sigma\}$ is the stress vector and $\{\varepsilon\}$ is the strain vector.

The concrete gravity dam's monoliths, usually unkeyed or lightly grouted, are expected to vibrate independently under severe ground excitations. So, two-dimensional plane stress idealization seems to be appropriate for the nonlinear seismic response study of concrete gravity dams. By assuming two-dimensional plane stress idealization, $[D]$ could be written as:

$$[D] = \frac{E}{1-\nu^2}\begin{bmatrix} 1 & \nu & 0 \\ \nu & 1 & 0 \\ 0 & 0 & \frac{1-\nu}{2} \end{bmatrix}. \quad (4)$$

3.2. Crack initiation and propagation criteria of concrete

The compressive stresses in concrete gravity dams are expected to be low, even under severe ground excitations, so, linear elastic behavior is assumed for the concrete of gravity dams under compressive loading. In contrast, the initiation of new cracks is assumed in concrete gravity dams when the principal tensile stress reaches the tensile strength of concrete. Tensile energy density was used as criteria for crack initiation and propagation in an element. An element will crack if the tensile energy density, $\frac{\sigma_1\varepsilon_1}{2}$, reaches the U_0 value as follows:

$$\frac{1}{2}\sigma_1\varepsilon_1 = U_0 = \frac{\sigma_i^2}{2E}; \qquad (\sigma_1 > 0), \quad (5)$$

where σ_1 and ε_1 are the major principal stress and strain, respectively, and σ_i is the apparent tensile strength of concrete [7].

3.3. Constitutive relationship during softening for concrete

A linear softening branch of concrete is assumed and the principle of conservation of energy should be conserved. By considering these two important factors,

the slope of softening branches of concrete determined, such as the energy released per area, will remain constant. At last, in finite element analysis, the final strains of no tensile resistance are defined as:

$$\varepsilon_f = \frac{2G_f}{\sigma_0 l_c}, \qquad \varepsilon'_f = \frac{2G'_f}{\sigma'_0 l_c}, \tag{6}$$

where ε_f, G_f, σ_0 and l_c are final strains, fracture energy, tensile strength of concrete and characteristic length of element, respectively [7]. Parameters with prime notation indicate corresponding values for dynamic analysis.

For formulating the softening behavior of concrete, a tangent modulus stiffness technique was used. In this method, the stiffness matrix was obtained by an incremental stress-strain relationship, and the constitutive matrix, relating the local stresses to local strains, is defined as [7]:

$$[D]_{np} = \frac{E}{1-\eta\nu^2}\begin{bmatrix} \eta & \eta\nu & 0 \\ \eta\nu & 1 & 0 \\ 0 & 0 & \mu\frac{1-\eta\nu}{2(1+\nu)} \end{bmatrix} \eta = \frac{E_n}{E}, \tag{7}$$

where parameter η is the ratio between the softening Young's modulus, E_n, in the direction normal to a fracture plane, E is the initial isotropic elastic modulus, and μ is the shear resistance factor. These parameters are shown in Figure 1.

A coaxial rotating crack model is considered, with respect to the orientation of crack bands, in finite element analysis. Thus, strains ε_n and ε_p are, respectively, ε_1, and ε_2, at the newly oriented material reference state. Using an implicit definition of the softened shear modulus in cracked elements, parameter μ is defined as follow:

$$\mu = \frac{1+\nu}{1-\eta\nu^2}\left(\frac{\eta\varepsilon_n - \varepsilon_p}{\varepsilon_n - \varepsilon_p} - \eta\nu\right) \qquad 0 \le \mu \le 1. \tag{8}$$

Here, ε_n and ε_p are the normal strain components in the directions normal and parallel to the fracture plane, respectively.

The local constitutive relationship matrix, $[D_{np}]$, can be transformed to the global coordinate directions as follows:

$$[D_{xy}] = [T]^T [D]_{np} [T], \tag{9}$$

where $[T]$ is the strain transformation matrix, defined as follows, in terms of the inclination of the normal to its crack plane (θ).

$$[T] = \begin{bmatrix} \cos^2\theta & \sin^2\theta & \sin\theta\cos\theta \\ \sin^2\theta & \cos^2\theta & -\sin\theta\cos\theta \\ -2\sin\theta\cos\theta & 2\sin\theta\cos\theta & \cos^2\theta - \sin^2\theta \end{bmatrix}. \tag{10}$$

3.4. Constitutive model for foundation

The elastic behavior of the foundation is discussed in the previous section. For higher levels of loading, when stresses in the foundation are beyond the elastic limit, a plasticity theory was used for modeling the behavior of the foundation.

3.4.1. Elasto-plastic behavior considered for rock masses

The elastoplastic constitutive relation of incremental stress-strain in the foundation in the plastic region is considered as [8]:

$$d\sigma_{ij} = \left(D_{ijkl} - \frac{D_{ijmn}\frac{\partial F}{\partial \sigma_{mn}}\frac{\partial Q}{\partial \sigma_{rs}}D_{rskl}}{\frac{\partial F}{\partial \sigma_{mn}}D_{mnrs}\frac{\partial Q}{\partial \sigma_{rs}} + m\frac{\partial Q}{\partial \sigma_{rs}}\sigma_{rs}}\right) d\varepsilon_{kl} = D^{ep}_{ijkl} d\varepsilon_{kl}, \tag{11}$$

which denotes the yielding function as $F(\sigma_{ij}, m)$ and the plastic potential function as $Q(\sigma_{ij})$, respectively, where m is a scalar function representing work-hardening or work softening.

4. Foundation modeling for dynamic analysis

The Mohr-Coulomb criterion is used as the yield function and the plastic potential function [8]. Yield function and plastic potential function are assumed to be the same. With this assumption, the stiffness matrix is symmetric and calculation is much easier. The foundation behavior in the plastic region is assumed to have no hardening or softening.

4.1. Stiffness matrix used for modeling the foundation

Because of the two dimensional analyses assumption, the stiffness matrix in the two dimensional coordinate is obtained as [8]:

$$\begin{Bmatrix} d\sigma_{xx} \\ d\sigma_{yy} \\ d\tau_{xy} \end{Bmatrix} = \begin{bmatrix} D^{ep}_{11} & D^{ep}_{12} & D^{ep}_{13} \\ D^{ep}_{21} & D^{ep}_{22} & D^{ep}_{23} \\ D^{ep}_{31} & D^{ep}_{32} & D^{ep}_{33} \end{bmatrix} \begin{Bmatrix} d\varepsilon_{xx} \\ d\varepsilon_{yy} \\ d\varepsilon_{xy} \end{Bmatrix}, \tag{12}$$

$$D^{ep}_{ij} = D_{ij} - \frac{1}{H}\left(\sum_{k=1}^{3} f_k D_{ik}\right)\left(\sum_{k=1}^{3} q_k D_{kj}\right), \tag{13}$$

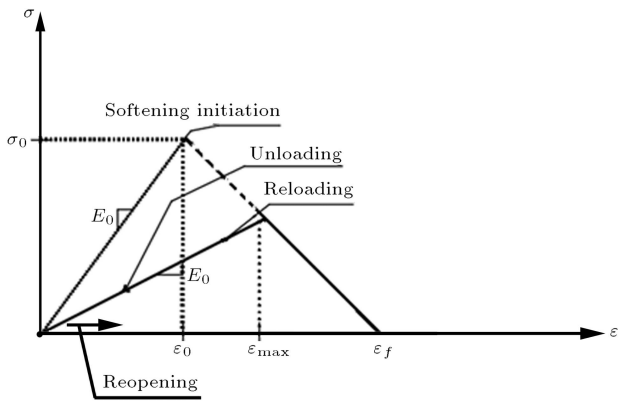

Figure 1. Stress-strain relationship for concrete.

where:

$$[D]=\frac{E}{1-\nu^2}\begin{bmatrix}1 & \nu & 0\\ \nu & 1 & 0\\ 0 & 0 & \frac{1-\nu}{2}\end{bmatrix}=\begin{bmatrix}D_{11} & D_{12} & D_{13}\\ D_{21} & D_{22} & D_{23}\\ D_{31} & D_{32} & D_{33}\end{bmatrix}, \quad (14)$$

and:

$$H=\sum_{k=1}^{3}\left[q_k\sum_{l=1}^{3}f_l D_{lk}\right]+m(q_1\sigma_{xx}+q_2\sigma_{yy}+q_3\tau_{xy}), \quad (15)$$

$$f_k=\frac{\partial F}{\partial \sigma_k}, \quad (16)$$

$$q_k=\frac{\partial Q}{\partial \sigma_k}. \quad (17)$$

In this study, there is no hardening or softening for the foundation behavior, so, $m=0$. The Mohr-Coulomb criterion is used for the yield and plastic potential function, as:

$$\tau=C-\sigma_n\tan\varnothing. \quad (18)$$

In the above equation, τ is the critical shear stress, σ_n is the normal stress acting over the failure plane, $\varnothing$ is the angle of internal friction and C is the inherent shear strength or cohesion of the material. Writing the Mohr-Coulomb criterion according to principal stresses, then, equations for yielding function and plastic potential function become:

$$F=Q=\frac{1+\sin\phi}{1-\sin\phi}\times(\sigma_{\max})-\sigma_{\min}-\frac{2\times C\times\cos\phi}{1-\sin\phi}, \quad (19)$$

$$\sigma_{\max}=\frac{\sigma_x+\sigma_y}{2}+\sqrt{\left(\frac{\sigma_x-\sigma_y}{2}\right)^2+{\tau_{xy}}^2}, \quad (20)$$

$$\sigma_{\min}=\frac{\sigma_x+\sigma_y}{2}-\sqrt{\left(\frac{\sigma_x-\sigma_y}{2}\right)^2+{\tau_{xy}}^2}. \quad (21)$$

f_k and q_k could be calculated as below:

$$f_1=q_1=\frac{\partial F}{\partial \sigma_x}=\frac{\sin\phi}{2}-\frac{\frac{\sigma_x-\sigma_y}{4}}{\sqrt{\left(\frac{\sigma_x-\sigma_y}{2}\right)^2+{\tau_{xy}}^2}}, \quad (22)$$

$$f_2=q_2=\frac{\partial F}{\partial \sigma_y}=\frac{\sin\phi}{2}+\frac{\frac{\sigma_x-\sigma_y}{4}}{\sqrt{\left(\frac{\sigma_x-\sigma_y}{2}\right)^2+{\tau_{xy}}^2}}, \quad (23)$$

$$f_3=q_3=\frac{\partial F}{\partial \tau_{xy}}=-\frac{\tau_{xy}}{\sqrt{\left(\frac{\sigma_x-\sigma_y}{2}\right)^2+{\tau_{xy}}^2}}. \quad (24)$$

5. Foundation boundary conditions

In this study, there are two different boundary conditions for the foundation: flexible mass-less foundation model and flexible massed foundation with Lysmer boundary condition. In the first model, the foundation was assumed massless. There is some rollers at the side of the foundation and it is fixed at the bottom [9,10]. For a massed foundation, some horizontal and vertical dampers are used at the side of the foundation and there are some rollers at the bottom of the modeled foundation [11]. Figures 2 and 3 illustrate these two different boundary conditions.

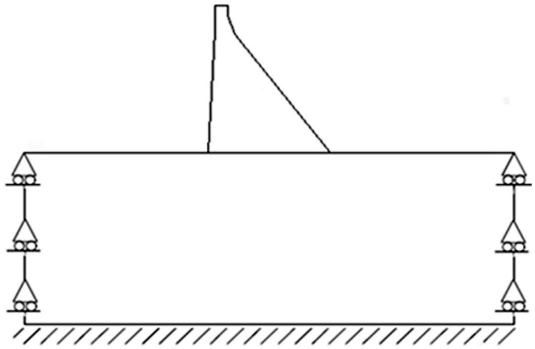

Figure 2. Boundary condition in massed foundation.

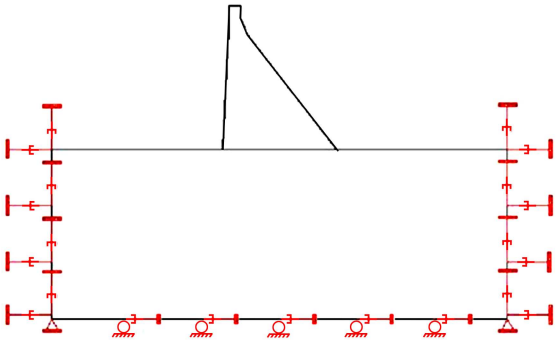

Figure 3. Boundary condition in massless foundation.

6. Analysis

The tallest monolith of a pine flat dam is used for the purpose of nonlinear dynamic analysis. The height of the tallest monolith is 122 m [12]. The length of the foundation from each side of the body of the dam is 126 m and the depth of the foundation is taken to be 126 m (Figure 4).

Properties of the dam concrete and properties of the rock foundation are shown in Tables 1 and 2 [12]. The wave reflection coefficient, due to sedimentation at the bottom of the reservoir, and the velocity of the pressure wave in the reservoir are taken as 0.82 and 1438.66 m/sec, respectively.

For performing dynamic analysis, the finite element program, NSAG-DRI, is used [13]. The program was developed for the nonlinear dynamic analysis of the dam-reservoir problem. In this study, NSAG-DRI was modified to include foundation nonlinearity by

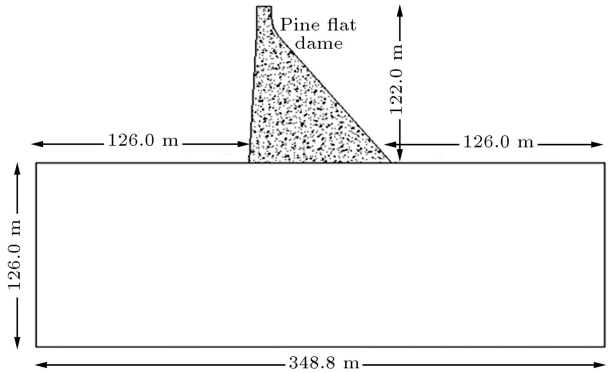

Figure 4. Geometric configuration of the dam body and foundation.

Table 1. Concrete material properties.

Elastic modulus	27580 MPa
Poisson's ratio	0.2
Unit weight	24357 N/m^3
Static fracture energy	300 N/m
Static tensile strength	2.4 MPa
Dynamic magnification factor	1.2

Table 2. Foundation material properties.

Elastic modulus	22400 MPa
Poisson's ratio	0.33
Unit weight	25928 N/m^3

considering the elastoplastic constitutive model. Four-node isoparametric elements are used for modeling the body of the dam, the foundation and the fluids. There are 5664 nodes and 5512 elements in the finite element model of the body of the dam and foundation, 3759 nodes of which are for the foundation. This finite element model is shown in Figure 5.

In the finite element formulation of the reservoir, the Sharan boundary condition is applied to the truncated reservoir at a distance equal to 10 times the dam height from the upstream face, and it is illustrated in Figure 6 [14].

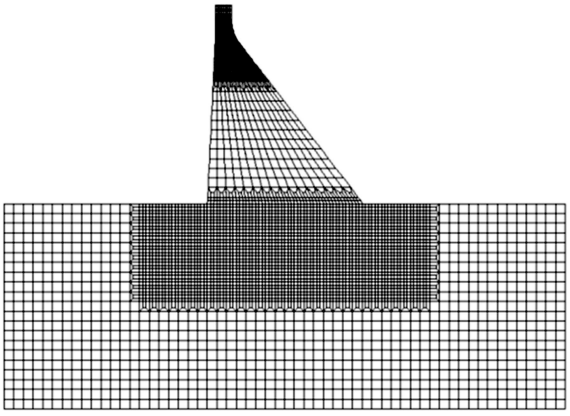

Figure 5. Finite element mesh of Pine Flat dam.

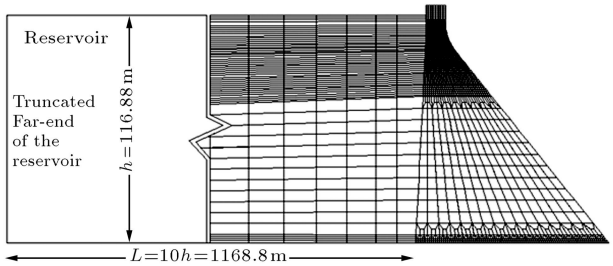

Figure 6. Finite element mesh of the reservoir.

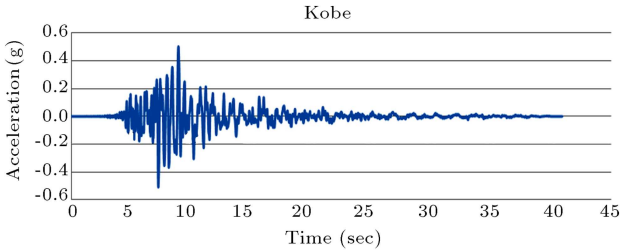

Figure 7. Horizontal component of 1995 Kobe earthquake.

The recorded ground acceleration of the 1995 Kobe earthquake with peak acceleration of 0.51 g is applied [15]. The recorded ground motion is shown in Figure 7. The effects of horizontal ground shaking with static gravity loads and hydrostatic pressure are considered in these analyses.

In this paper, 9 different cases are investigated. In all cases, the smeared crack model is used for the dam body. In each case, depending on the model, different assumptions are made for the foundation and dynamic loading. Table 3 shows all different cases of the analysis and their assumptions.

7. Numerical results

Nonlinear dynamic analysis of the dam-reservoir-foundation system was carried out considering different cases of the system. Generally, it is shown that the cracking pattern of a dam usually starts with the cracking of the first element on the interface of the dam and reservoir at the upstream face. This crack will propagate into the dam body later in the process of dynamic analysis. The next crack profile of the dam body is near the slope discontinuity. The crack (damage) profiles inside the foundation, dependent on the assumption adopted for cases, are different.

7.1. Case 1

In this case, the smeared cracking model is used for the massed foundation (Static tensile strength=4.6 MPa). The earthquake is applied to the foundation boundaries, and total stresses are used for calculating foundation responses. Crack profiles of Case 1 are illustrated in Figure 8.

The analysis was carried out for different parame-

Table 3. Different cases for foundation in the analysis.

Case 1	Smeared model (foundation)	Massed foundation	Total stress	Static tensile strenght=4.6 MPa	Earthquake at the foundation boundaries
Case 2	Elastoplastic model (foundation)	Massed foundation	Total stress	$\varnothing = 47$ deg, $C = 0.6$ MPa	Earthquake at foundation boundaries
Case 3	Elastoplastic model (foundation)	Massed foundation	Effective stress	$\varnothing = 47$ deg, $C = 0.6$ MPa	Earthquake at foundation boundaries
Case 4	Elastoplastic model (foundation)	Massed foundation	Total stress	$\varnothing = 47$ deg, $C = 0.6$ MPa	Earthquake at dam foundation interface
Case 5	Elastoplastic model (foundation)	Massed foundation	Effective stress	$\varnothing = 47$ deg, $C = 0.6$ MPa	Earthquake at dam foundation interface
Case 6	Elastoplastic model (foundation)	Massless foundation	Total stress	$\varnothing = 47$ deg, $C = 0.6$ MPa	Earthquake at foundation boundaries
Case 7	Elastoplastic model (foundation)	Massless foundation	Effective stress	$\varnothing = 47$ deg, $C = 0.6$ MPa	Earthquake at foundation boundaries
Case 8	Elastoplastic model (foundation)	Massless foundation	Total stress	$\varnothing = 47$ deg, $C = 0.6$ MPa	Earthquake at dam foundation interface
Case 9	Elastoplastic model (foundation)	Massless foundation	Effective stress	$\varnothing = 47$ deg; $C = 0.6$ MPa	Earthquake at dam foundation interface

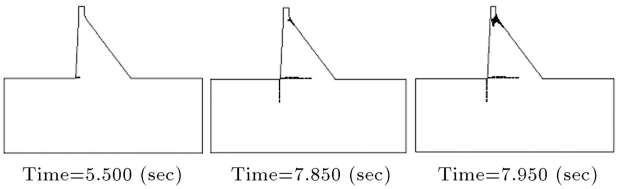

Figure 8. Crack profiles of Case 1 (smeared model; massed foundation; total stresses; static tensile strength=4.6 MPa; earthquake at foundation boundaries).

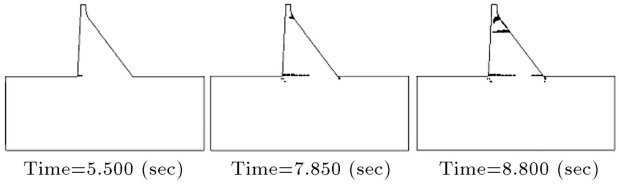

Figure 9. Crack profiles of Case 2 (elastoplastic model; massed foundation; total stress; $\varnothing = 47$ deg; $C = 0.6$ MPa; earthquake at foundation boundaries).

ters of foundation nonlinearity, considering the smeared crack model. Based on the crack profile from all analyses, it was found that the smeared crack model for the foundation is not appropriate, knowing that the failure mode in the foundation is the shear failure mode.

The crack patterns for all analyses are more or less the same as Case 1 for the foundation. Generally, foundation cracking starts at the upstream and propagates vertically into the foundation for a wide range of parameters of the model.

7.2. Case 2

The elastoplastic model is used for the massed foundation, and the earthquake is applied to the foundation boundaries. Total stresses are used for calculating foundation responses, and friction angle and cohesion are taken as 47 degree and 0.6 MPa, respectively. Crack profiles of Case 2 are illustrated in Figure 9. When the elastoplastic model is used for the foundation, the intensity of damage to the body of the dam is lower in comparison to the condition when the smeared model is used. The analysis was stopped earlier in Case 1 compared to Case 2 because of the high intensity of occurred damage.

This fact can be interpreted by the energy that dissipated in each case. Considering the smeared model for the foundation, the amount of energy dissipated in each cycle of loading in the foundation is less than the case of the elastoplastic model for the foundation.

7.3. Case 3

In this case, the elastoplastic model is used for the massed foundation, and the earthquake is applied to the foundation boundaries. Effective stresses are used for calculating foundation responses, and the friction angle and cohesion are 47 degree and 0.6 MPa, respectively. Crack profiles of Case 3 are illustrated in Figure 10.

Results show that employing effective stresses instead of total stresses gives a more realistic response. Using effective stresses in the analysis, there are more elements of the foundation in the plastic region.

7.4. Case 4

In this case, the elastoplastic model is used for the massed foundation, and the earthquake is inserted into the dam foundation interface. Total stresses are used for calculating foundation responses, and the friction angle and cohesion are 47 degree and 0.6 MPa,

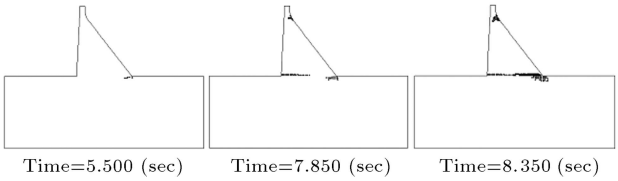

Figure 10. Crack profiles of Case 3 (elastoplastic model; massed foundation; effective stress; $\varnothing = 47$ deg; $C = 0.6$ MPa; earthquake at foundation boundaries).

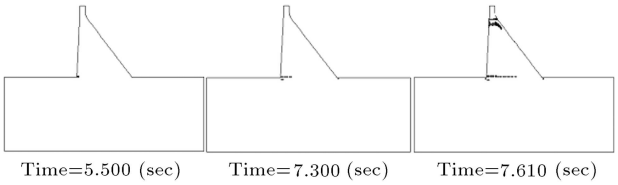

Figure 11. Crack profiles of Case 4 (elastoplastic model; massed foundation; total stress; $\varnothing = 47$ deg; $C = 0.6$ MPa; earthquake at dam foundation interface).

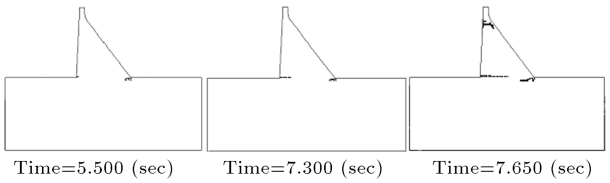

Figure 12. Crack profiles of Case 5 (elastoplastic model; massed foundation; effective stress; $\varnothing = 47$ deg; $C = 0.6$ MPa; earthquake at dam foundation interface).

respectively. Crack profiles of Case 4 are illustrated in Figure 11.

7.5. Case 5

In this case, the elastoplastic model is used for the massed foundation, and the earthquake is inserted into the dam foundation interface. Effective stresses are used for calculating foundation responses, and the friction angle and cohesion are 47 degree and 0.6 MPa, respectively. Crack profiles of Case 5 are illustrated in Figure 12.

When the earthquake is inserted into the massed foundation boundaries instead of the dam-massed foundation interface, the intensity of damage to the body of the dam is lower. The analysis stopped earlier in Case 5 compared to Case 3 because of the high intensity of occurred damage in the body of the dam, but at the end of the analysis, there were fewer elements in the plastic region for the case in which the earthquake was applied to the dam-foundation interface.

When the earthquake is inserted into the massed foundation boundaries, there are more effects of energy absorption in the foundation of the elements. Therefore, the number of plastic elements of the foundation will increase and the foundation absorbs more energy into plastic region. So, it will reduce the amount of damage to the dam body, but there are more plastic elements in the foundation at the end of the analysis.

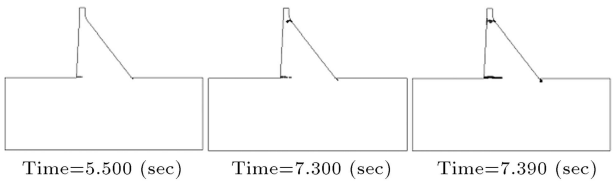

Figure 13. Crack profiles of Case 6 (elastoplastic model; massless foundation; total stress; $\varnothing = 47$ deg; $C = 0.6$ MPa; earthquake at foundation boundaries).

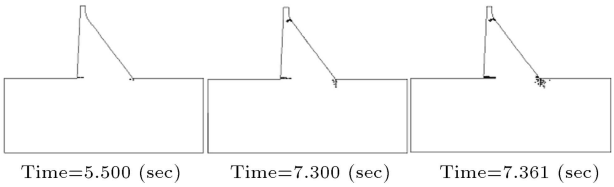

Figure 14. Crack profiles of Case 7 (elastoplastic model; massless foundation; effective stress; $\varnothing = 47$ deg; $C = 0.6$ MPa; earthquake at foundation boundaries).

7.6. Case 6

In this case, the elastoplastic model is used for the massless foundation, and the earthquake is inserted into the foundation boundaries. Total stresses are used for calculating foundation responses, and the friction angle and cohesion are 47 degree and 0.6 MPa, respectively. Crack profiles of Case 6 are illustrated in Figure 13.

7.7. Case 7

In this case, the elastoplastic model is used for the massless foundation, and the earthquake is inserted into the foundation boundaries. Effective stresses are used for calculating foundation responses, and the friction angle and cohesion are 47 degree and 0.6 MPa, respectively. Crack profiles of Case 7 are illustrated in Figure 14. Using a massed foundation and considering its inertia and energy absorption, the intensity of damage to the dam body reduces.

7.8. Case 8

The elastoplastic model is used for the massless foundation, and the earthquake is inserted into the dam foundation interface. Total stresses are used and friction angle and cohesion are 47 degree and 0.6 MPa, respectively. Crack profiles of Case 8 are illustrated in Figure 15.

7.9. Case 9

The elastoplastic model is used for the massless foundation, and the earthquake is inserted in the dam foundation interface. Effective stresses are used and friction angle and cohesion are 47 degree and 0.6 MPa,

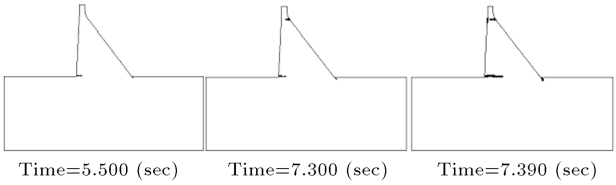

Figure 15. Crack profiles of Case 8 (elastoplastic model; massless foundation; total stress; $\varnothing = 47$ deg; $C = 0.6$ MPa; earthquake at dam foundation interface).

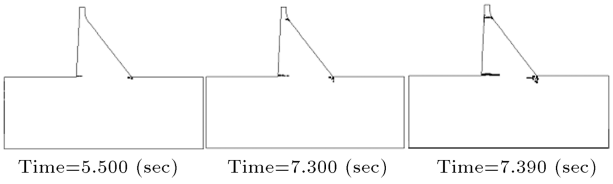

Figure 16. Crack profiles of Case 9 (elastoplastic model; massless foundation; effective stress; $\varnothing = 47$ deg; $C = 0.6$ MPa; earthquake at dam foundation interface).

respectively. Crack profiles of Case 9 are illustrated in Figure 16.

As shown in the massless foundation, there is no remarkable difference between inserting the earthquake in the dam-foundation interface or at the foundation boundaries. For a massless foundation, the velocity of wave propagation in the foundation would be infinite, which is equivalent to inserting the earthquake in the dam-foundation boundaries. Therefore, it necessitates ignoring foundation inertia and energy radiation in all massless foundation cases.

8. Conclusion

The nonlinear dynamic analysis of a concrete gravity dam was carried out to investigate the effects of foundation behavior and its boundary conditions on the responses. There are two different constitutive models for the foundation behavior in this study: a smeared model and an elastoplastic model, but it was mainly focused on the effect of foundation nonlinearity, based on the elastoplastic model. Using the smeared crack model in comparison to a elastoplastic model, with the Mohr-coulomb criterion as the yield and plastic potential function, is not appropriate for the foundation, knowing that the failure mode in the foundation is the shear failure mode, and elements of the foundation are expected to behave realistically when an elastoplastic model is considered for them. Results show that when an elastoplastic model is used for the foundation, the intensity of damage to the body of the dam is lower due to the higher dissipated energy in each cycle in comparison with the smeared crack model.

Responses of the model using total stresses and effective stresses were obtained, considering the elastoplastic model for the foundation. Using effective stresses and reducing pore pressure from total stresses can result in more plastic elements in the foundation. Considering a massed foundation will reduce the intensity of damage to the dam body in comparison to a massless foundation, because of inertia and energy absorption in the massed foundation, which is ignored in massless foundations. There are two different approaches for inserting earthquake excitation. An earthquake can be inserted at the foundation boundaries or at the dam foundation interface. Inserting an earthquake into the massed foundation boundaries, compared with the case where the earthquake is inserted in the dam-massed foundation interface, can give different crack patterns. When an earthquake is applied to the massed foundation boundaries, the intensity of damage to the dam body will reduce, but at the end of the analysis, there are more elements of the foundation in the plastic region. This can be interpreted as being due to higher energy absorption in the foundation plastic element. For a massless foundation, because of the infinite velocity of wave propagation in the foundation, there is no significant difference in the crack patterns for these two methods of loading; the crack patterns are approximately the same.

References

1. Rescher, O.R. "Importance of cracking in concrete dams", *J. of Eng. Fracture Mech.*, **35**(1/2/3), pp. 503-524 (1990).
2. Motamedi, M.H., Amini, A. and Ghaemian, M. "The study of the foundation role in the seismic nonlinear behavior of concrete gravity dams", *14th World Conf. on Earthquake Eng.* (2008).
3. Sarkar, R., Paul, D.K. and Stempniewski, L. "Influence of reservoir and foundation on the nonlinear dynamic response of concrete gravity dams", *ISET J. of Earthquake Tech.*, Paper No 490, **44**(2), pp. 377-389 (June 2007).
4. Arabshahi, H. and Lotfi, V. "Earthquake response of concrete gravity dams including dam-foundation interface nonlinearities", *J. of Eng. Structures*, **30**, pp. 3065-3073 (2008).
5. Fishman, Y.A. "Features of shear failure of brittle materials and concrete structures on rock foundation", *J. of Rock Mech. and Mining Sci.*, **45**, pp. 976-992 (2008).
6. Ghaemian, M. and Ghobarah, A. "Staggered solution schemes for dam-reservoir interaction", *J. of Fluid and Structures*, **12**, pp. 933-948 (1998).
7. Bhattacharjee, S.S. and Leger, P. "Seismic cracking and energy dissipation in concrete gravity dams", *J. of Earthquake Eng. & Structural Dynamics*, **22**, pp. 991-1007 (1993).

8. Jing, L. and Stephansson, O., *Fundamentals of Discrete Element Methods for Rock Engineering Theory and Applications*, Elsevier Sci., **85**, pp. 87-94 (2007).
9. US. Army Corps of Engineers (USACE) "Time-history dynamic analysis of concrete hydraulic structures", Chapter 2, *Analytical Modeling of Concrete Hydraulic Structures, 3-Time-History Numerical Solution Techniques*, EM 1110-2-6051 (2003).
10. US. Army Corps of Engineers (USACE) "Earthquake design and evaluation of concrete hydraulic structures", Chapter 4, *Methods of Seismic Analysis and Structural Modeling*, EM-1110-2-6053 (2007).
11. Lysmer, J. and Kuhlemyer, R.L. "Finite dynamic model for infinite media", *J. of Eng. Mech. Division, ASCE*, **95**, pp. 859-877 (1969).
12. Ghaemian, M. and Ghobarah, A. "Nonlinear seismic analysis of concrete gravity dams including dam-reservoir interaction", *J. of Eng. Structures*, **21**, pp. 306-315 (1999).
13. Ghaemian, M. "Manual of NSAG-DRI, a computer programfor nonlinear seismic analysisof gravity dams including dam-reservoir-foundation interaction", available at Sharif.edu/∼ghaemian (2008).
14. Sharan, S. "Finite element analysis of unbounded and incompressible fluid domains", *Int. J.of Numerical Methods in Eng.*, **21**, pp. 1659-1669 (1985).
15. PEER Strong Motion Database, http://www.peer.berkeley.edu.

Biographies

Seyyed Meisam Aghajanzadeh was a graduate student in the Civil Engineering Department of Sharif University of Technology, Tehran, Iran, from 2012-2013. His research interests include: the seismic response of concrete gravity dams under seismic loadings, and the effects of dam-foundation interaction on the seismic response of concrete gravity dams using different nonlinear constitutive models.

Mohsen Ghaemian is Associate Professor in the Civil Engineering Department at Sharif University of Technology, Tehran, Iran. His research interests include: dynamic responses of gravity and arch dams, dam-reservoir-foundation interaction effects, seismic response of dams due to non-uniform excitations and nonlinear behavior of concrete dams.